Tetrahedron 66 (2010) 3842–3848

Contents lists available at ScienceDirect

Tetrahedron

journal homepage: www.elsevier.com/locate/tet

Colorimetric and fluorometric sensing of the Lewis acidity of a metal ion by metal-ion complexation of imidazo[1,2-*a*]pyrazin-3(7*H*)-ones

Takashi Hirano [a,*], Takashi Sekiguchi [a], Daisuke Hashizume [b], Hiroshi Ikeda [c,d], Shojiro Maki [a], Haruki Niwa [a]

[a] *Department of Applied Physics and Chemistry, The University of Electro-Communications, Chofu, Tokyo 182-8585, Japan*
[b] *Advanced Technology Support Division, RIKEN, Wako, Saitama 351-0198, Japan*
[c] *Department of Applied Chemistry, Graduate School of Engineering, Osaka Prefecture University, Sakai, Osaka 599-8531, Japan*
[d] *The Research Institute for Molecular Electronic Devices (RIMED), Osaka Prefecture University, Sakai, Osaka 599-8531, Japan*

ARTICLE INFO

Article history:
Received 16 January 2010
Received in revised form
11 March 2010
Accepted 12 March 2010
Available online 18 March 2010

Keywords:
Metal-ion complex
Lewis acidity
Absorption spectrum
Fluorescence

ABSTRACT

Metal-ion complexation of 7-benzylimidazo[1,2-*a*]pyrazin-3(7*H*)-one derivative (**2**) with Li^+, Mg^{2+}, Ca^{2+}, Ba^{2+}, Sc^{3+}, and La^{3+} in acetonitrile resulted in successive modulations of its UV/vis absorption and fluorescence spectroscopic properties. This result indicates that **2** can be used as a colorimetric and fluorometric sensor of the Lewis acidity of a metal ion in aprotic solutions. The hypothesis that the metal-ion complex has a O10(imidazopyrazinone)–metal ion bond was supported by X-ray crystallographic analysis and quantum chemical calculations for a Li^+ complex of 7-methylimidazo[1,2-*a*]pyrazin-3(7*H*)-one derivative (**1**).

1. Introduction

In recent decades, colorimetric and fluorometric sensors have been used in various scientific fields.[1] In biology, for instance, such sensors are useful reagents for living cell imaging. It is important to design novel sensors because they have the potential to overcome many technical limitations in experiments. Imidazo[1,2-*a*]pyrazin-3(7*H*)-one (imidazopyrazinone, Chart 1) often is used as a bioluminescent substrate,[2] and it is an attractive core structure for useful sensors. We previously developed a series of imidazopyrazinone derivatives, including 7-methyl-2-phenylimidazo[1,2-*a*]pyrazin-3(7*H*)-one (**1b**) and structurally related compounds. We demonstrated that the solvent effect on absorption and fluorescent properties of **1b** is induced by a hydrogen-bonding interaction in which a protic solvent molecule and **1b** act like a Brönsted acid and base, respectively.[3] These findings lead us to further study of complexation of imidazopyrazinone with a metal ion (M^{n+}) revealing that M^{n+} and imidazopyrazinone act as a Lewis acid and base, respectively.

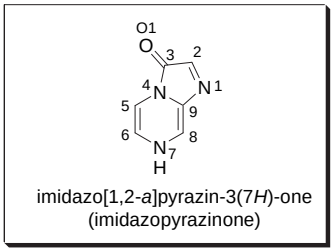

imidazo[1,2-*a*]pyrazin-3(7*H*)-one
(imidazopyrazinone)

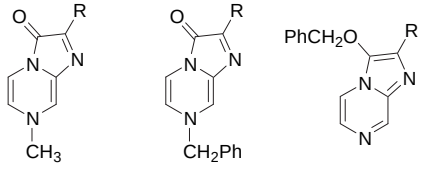

1a: R = CH_3
1b: R = Ph

2a: R = CH_3
2b: R = Ph

3a: R = CH_3
3b: R = Ph

Chart 1.

In this study, we prepared a new series of imidazopyrazinones [7-benzylimidazo[1,2-*a*]pyrazin-3(7*H*)-one derivatives (**2**, Chart 1)] and studied their absorption and fluorescent properties in the presence of various metal ions (M^{n+}).[4,5] We found that **2** and M^{n+} form a metal-ion complex, and the UV/vis absorption and fluorescence

* Corresponding author. Tel.: +81 42 443 5489; fax: +81 42 486 1966; e-mail address: hirano@pc.uec.ac.jp (T. Hirano).

0040-4020/$ – see front matter © 2010 Elsevier Ltd. All rights reserved.
doi:10.1016/j.tet.2010.03.043

spectra of this complex vary depending on the Lewis acidity of M^{n+}. The structure of the metal-ion complex was analyzed using X-ray crystallography and quantum chemical calculations for a Li^+ complex of **1**. As a result, we were able to clarify the relationship between the spectroscopic property and the structural characteristics of the metal–ion complex of an imidazopyrazinone, and provide the basis of the application of imidazopyrazinones as colorimetric and fluorometric sensors of the Lewis acidity of a metal ion.

2. Results and discussion

2.1. Spectroscopic properties of the metal-ion complexes of imidazopyrazinones 2

Benzylimidazopyrazinones **2** were prepared by benzylation of the corresponding NH derivatives (**4**) together with benzyloxyimidazopyrazines **3**, which are structurally related reference compounds that have a different π electronic character.[4] UV/vis absorption and fluorescence spectra of complexes of **2** with a series of metal ions (Li^+, Mg^{2+}, Ca^{2+}, Ba^{2+}, Sc^{3+}, and La^{3+}) were measured in acetonitrile at 25 °C (Figs. 1 and 2). Perchlorate salts of Li^+, Mg^{2+}, Ca^{2+}, and Ba^{2+} and trifluoromethanesulfonate salts of Sc^{3+} and La^{3+} were used in this experiment. We have also investigated the spectroscopic property of **2** in aqueous solutions containing the metal ions. Unfortunately, however, we were unable to observe a spectral change of **2** caused by metal-ion complex formation, indicating that hydrogen bond formation of **2** with water molecules occurs in preference to metal-ion complex formation.[3]

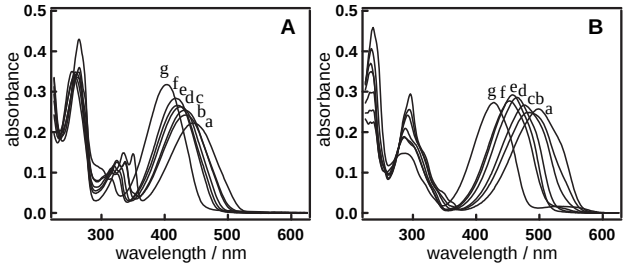

Figure 1. UV/vis absorption spectra of **2a** (2.4×10^{-5} mol L^{-1}) (A) and **2b** (1.4×10^{-5} mol L^{-1}) (B) in CH_3CN containing various metal ions at 25 °C: (a) free, (b) Li^+, (c) Ba^{2+}, (d) Ca^{2+}, (e) Mg^{2+}, (f) La^{3+}, and (g) Sc^{3+} (A: $[Li^+]=[Ba^{2+}]=[Ca^{2+}]=[Mg^{2+}]=0.025$ mol L^{-1} and $[La^{3+}]=[Sc^{3+}]=2.5\times10^{-4}$ mol L^{-1}; B: $[Li^+]=[Ba^{2+}]=[Ca^{2+}]=[Mg^{2+}]=0.010$ mol L^{-1} and $[La^{3+}]=[Sc^{3+}]=1.0\times10^{-4}$ mol L^{-1}).[4]

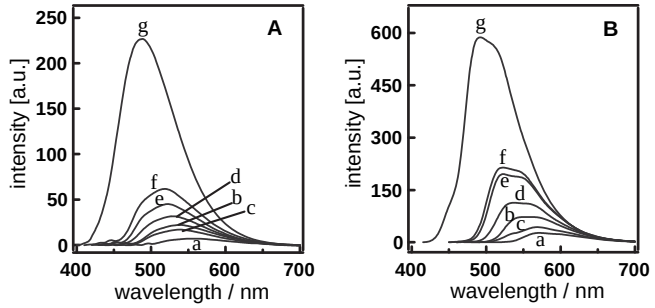

Figure 2. Fluorescence spectra of **2a** (2.5×10^{-6} mol L^{-1}) (A) and **2b** (1.0×10^{-6} mol L^{-1}) (B) in CH_3CN containing various metal ions at 25 °C: (a) free, (b) Li^+, (c) Ba^{2+}, (d) Ca^{2+}, (e) Mg^{2+}, (f) La^{3+}, and (g) Sc^{3+} (A: $[Li^+]=[Ba^{2+}]=[Ca^{2+}]=[Mg^{2+}]=0.025$ mol L^{-1} and $[La^{3+}]=[Sc^{3+}]=2.5\times10^{-4}$ mol L^{-1}; B: $[Li^+]=[Ba^{2+}]=[Ca^{2+}]=[Mg^{2+}]=0.010$ mol L^{-1} and $[La^{3+}]=[Sc^{3+}]=2.0\times10^{-4}$ mol L^{-1}).

Table 1 summarizes absorption maxima (λ_{ab}) of the lowest energy bands, the fluorescence emission maxima (λ_{fl}), and the fluorescence quantum yields (Φ_{fl}) of **2** and their metal-ion complexes. To evaluate the blue-shifted λ_{ab} and λ_{fl} values of the metal-ion complexes of **2**, we attempted to correlate the energy values (E_{ab} and E_{fl}) estimated from λ_{ab} and λ_{fl} with the Fukuzumi parameters for the Lewis acidity (ΔE) of the metal ions (Fig. 3).[6] The E_{ab}-versus-ΔE and E_{fl}-versus-ΔE plots for **2** show linear correlations [$E_{ab}=0.37\Delta E+2.69$ ($r=0.98$) and $E_{fl}=0.43\Delta E+2.08$ ($r=0.96$) for the metal-ion complexes of **2a**; $E_{ab}=0.55\Delta E+2.33$ ($r=0.97$) and $E_{fl}=0.60\Delta E+1.93$ ($r=0.94$) for the metal-ion complexes of **2b**]. This result indicates that the strength of the Lewis acid–base bond between **2** and a metal ion with the ΔE value determines the degree of the blue shifts of λ_{ab} and λ_{fl}. The slope of the $E_{ab}-\Delta E$ correlation for the **2b** complexes is larger than that for the **2a** complexes, and the intercept for the **2b** complexes is smaller than that for the **2a** complexes. Thus, the metal-ion complexes of the 2-phenyl derivative **2b** have a wider color variation range and a higher sensitivity to the Lewis acidity of the metal ions compared to those of the 2-methyl derivative **2a**. The slope of the $E_{fl}-\Delta E$ correlation for the **2b** complexes also is larger than that for the complexes of **2a**, whereas the difference in the intercepts between the complexes of **2a** and **2b** are small. In particular, the λ_{fl} values for the Sc^{3+} complexes of **2a** and **2b** are almost the same, whereas the λ_{ab} values for their Sc^{3+} complexes are different from each other. This result indicates that the imidazopyrazinone moiety in the Sc^{3+} complex of **2b** has no conjugation with the phenyl group at C2 in the excited singlet (S_1) state, but it has conjugation in the ground state. The Φ_{fl} values of the metal-ion complexes of **2** increase with an increase in the ΔE value of a metal ion. The Sc^{3+} complexes of **2** exhibited the largest Φ_{fl} values among the metal-ion complexes of **2**.

Table 1
Absorption maxima (λ_{ab}), fluorescence emission maxima (λ_{fl}), fluorescence quantum yields (Φ_{fl}), and formation constants (K)[a] for **2** and their metal-ion complexes in CH_3CN at 25 °C[b]

Metal ion (ΔE/eV)[c]	**2a**				**2b**			
	λ_{ab}/nm	λ_{fl}/nm	Φ_{fl}	K/mol^{-1} L	λ_{ab}/nm	λ_{fl}/nm	Φ_{fl}	K/mol^{-1} L
Free	447	559	0.01	—	500	571	0.03	—
Ba^{2+} (0.49)	431	540	0.02	1.1×10^3	476	557	0.09	5.6×10^2
Li^+ (0.53)	430	538	0.03	2.5×10^2	475	569	0.05	1.2×10^2
Ca^{2+} (0.58)	424	528	0.03	1.5×10^4	464	538	0.13	6.2×10^3
Mg^{2+} (0.65)	422	524	0.05	2.8×10^4	457	523	0.19	8.0×10^3
La^{3+} (0.82)	418	519	0.06	[d]	452	522	0.22	[d]
Sc^{3+} (1.00)	403	489	0.20	[d]	428	491	0.51	[d]

[a] The errors are within 8%.
[b] Ref. 4.
[c] The Fukuzumi parameter for the Lewis acidity from Ref. 6.
[d] Efficient complexation occurred in a stepwise manner.

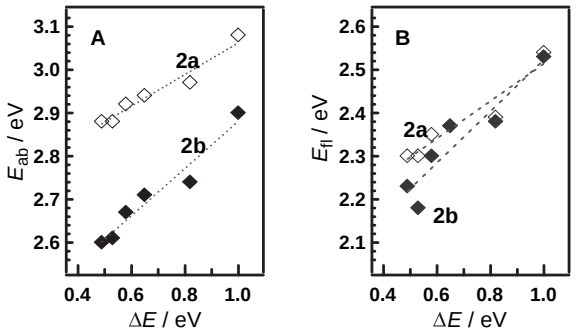

Figure 3. E_{ab} (A) and E_{fl} (B) values for the metal-ion complexes of **2** plotted as functions of the Lewis acidity ΔE.

Formation constants (K) of the metal-ion complexes were determined by analyzing the absorption spectral changes of **2** in the presence of Li^+, Mg^{2+}, Ca^{2+}, and Ba^{2+} on the assumption that **2** forms a 1:1 complex ($M^{n+}\cdot\mathbf{2}$) with M^{n+} [Eq. 1].

$$M^{n+} + \mathbf{2} \overset{K}{\rightleftarrows} M^{n+}\cdot\mathbf{2} \quad (1)$$

Figure 4 shows a typical example for complex formation of **2** in the presence of Mg^{2+} at various concentrations. The spectra showed isosbestic points and were nicely analyzed by nonlinear least squares curve fitting for the 1:1 equilibrium.[7] Estimated *K* values are summarized in Table 1. The order of the *K* values for the complexes of **2** (Mg^{2+}>Ca^{2+}>Ba^{2+}>Li^{+}) was determined mainly by the strength of the Lewis acidity of the metal ions, although the order of the *K* values of Li^{+} and Ba^{2+} was inverted.

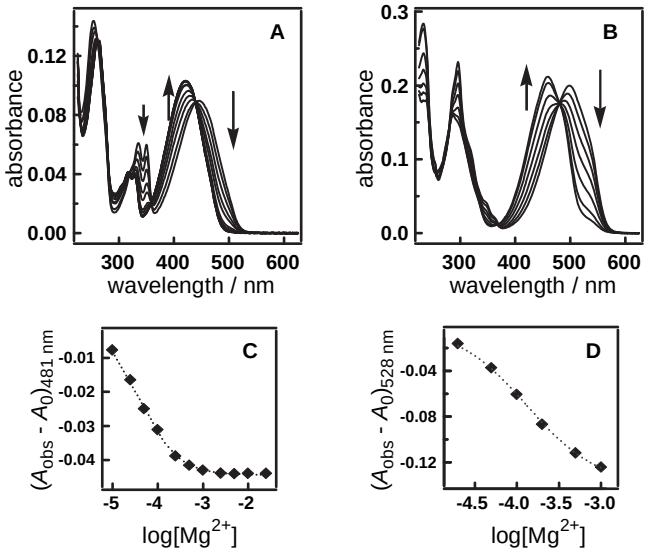

Figure 4. UV/vis absorption spectra of **2a** (9.7×10^{-6} mol L^{-1}) (A) and **2b** (1.1×10^{-5} mol L^{-1}) (B) in CH_3CN containing Mg^{2+} at various concentrations at 25 °C. The plot of $(A_{obs}-A_0)$ at 481 nm versus log [Mg^{2+}] for complexation of **2a** (C) and the plot of $(A_{obs}-A_0)$ at 528 nm versus log [Mg^{2+}] for complexation of **2b** (D) ([Mg^{2+}]=1.0×10^{-5}–0.025 mol L^{-1} for **2a** and [Mg^{2+}]=2.0×10^{-5}–0.010 mol L^{-1} for **2b**). The dotted lines in C and D are the fitted curves corresponding to 1:1 complexation.

Formation of the Sc^{3+} and La^{3+} complexes of **2** was more efficient than that of their Li^{+}, Mg^{2+}, Ca^{2+}, and Ba^{2+}complexes. The spectral changes for the complex formation of **2** in the presence of Sc^{3+} and La^{3+} at various concentrations indicate that several kinds of complexes are formed in a stepwise manner. Figure 5 shows typical spectra for Sc^{3+} complexation of **2**. In Sc^{3+} complexation with **2a** (2.4×10^{-5} mol L^{-1}), the 2:1 complex of **2a** and Sc^{3+} effectively formed at [Sc^{3+}]=0–1.0×10^{-5} mol L^{-1} with clear isosbestic points. A further increase of [Sc^{3+}] (>1.0×10^{-5} mol L^{-1}) resulted in a small blue shift of the lowest energy band, indicating that the 2:1 complexes of **2a** and Sc^{3+} transformed to another such as a 1:1 complex. A two-step spectral change of **2b** (2.4×10^{-5} mol L^{-1}) via Sc^{3+} complexation also was observed (Fig. 5C and D). Similarly, effective formation of the 2:1 complexes of **2** and La^{3+} was observed.

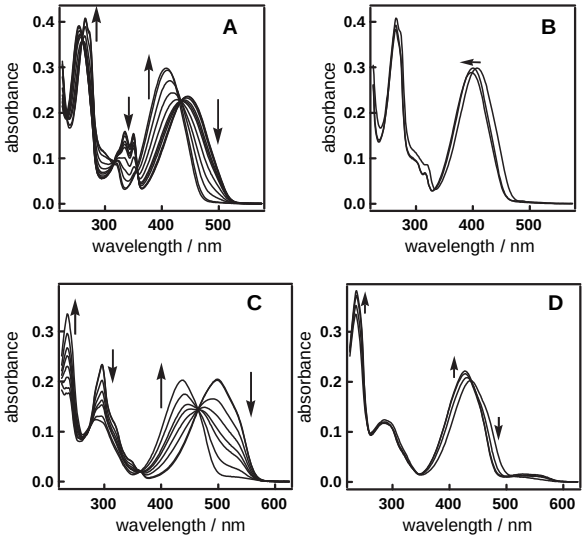

Figure 5. UV/vis absorption spectra of **2a** (2.6×10^{-5} mol L^{-1}) (A and B) and **2b** (1.1×10^{-5} mol L^{-1}) (C and D) in CH_3CN containing Sc^{3+} at various concentrations at 25 °C (A: [Sc^{3+}]=0–1.0×10^{-5} mol L^{-1}; B: [Sc^{3+}]=1.0–20×10^{-5} mol L^{-1}; C: [Sc^{3+}]=0–5.0×10^{-6} mol L^{-1}; D: [Sc^{3+}]=5.0–100×10^{-6} mol L^{-1}).

The spectroscopic properties of imidazopyrazines **3** and protonated species **2**H^{+} also were investigated in terms of their π electronic character. The lowest energy bands of **3a** and **3b** were observed at 324 (ε 4500 cm^{-1} mol^{-1} L) and 342 nm (ε 7500 cm^{-1} mol^{-1} L) in acetonitrile, respectively. Absorption spectra of **2a**H^{+} and **2b**H^{+} generated in acetonitrile containing methanesulfonic acid (2.5×10^{-3} mol L^{-1}) showed the lowest energy bands at 381 and 403 nm, respectively. The different π electronic character of the ring systems of **2**, **2**H^{+}, and **3** explains these observations.[3] The aromatic character of the 10π-electron system of the imidazopyrazine rings of **3** is stronger than that of the imidazopyrazinone rings of **2**, resulting in a blue shift of the λ_{ab} values of **3** compared to those of **2**. The aromatic character of the imidazopyrazium rings of **2**H^{+} is intermediate between those of the imidazopyrazinone rings of **2** and the imidazopyrazine rings of **3**, yielding λ_{ab} values of **2**H^{+} that are intermediate between those of **2** and **3**.

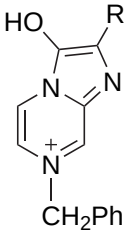

2aH^{+}: R = CH_3
2bH^{+}: R = Ph

We evaluated the π electronic character of the imidazopyrazinone moiety in the metal-ion complexes of **2** by comparing to that of the imidazopyrazinone ring of **2** and the imidazopyrazinium ring of **2**H^{+}. Because an imidazopyrazinone ring has a zwitterionic structure with localized negative charge at the O10 atom,[3] a metal–ion complex ($M^{n+}\cdot$**2**) will be formed by the coordination of the O10 atom of **2** to a metal ion (M^{n+}) (Scheme 1). Thus, it seems reasonable to describe the imidazopyrazinone moiety in $M^{n+}\cdot$**2** with resonance structures **I** and **II** (Scheme 1): **I** contains the parent imidazopyrazinone ring in the vicinity of M^{n+}, and **II** contains the imidazopyrazinium moiety. Because **II** has a structure similar to that of **2**H^{+}, an increase in the **II** character in $M^{n+}\cdot$**2** leads to a blue shift of the electronic absorption band of $M^{n+}\cdot$**2** compared to that of **2**. In fact, the λ_{ab} values of $M^{n+}\cdot$**2** are intermediate between those of **2** and **2**H^{+}. Therefore, the degree of the **II** character in $M^{n+}\cdot$**2** will determine the magnitude of the blue shift of the lowest energy absorption band.

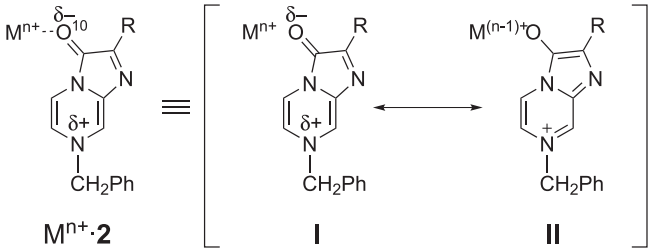

Scheme 1.

Imidazopyrazines **3a** and **3b** had the same λ_{fl} value at 420 nm in acetonitrile, which indicates that the phenyl group of **3b** does not participate in the π-electronic conjugation with the imidazopyrazine ring in the S_1 state. A similar non-conjugation of the phenyl group was observed in the Sc^{3+} complex of **2b** in the S_1 state. The Φ_{fl} values of **3a** and **3b** were 0.28 and 0.13, respectively, which are larger than those of the corresponding **2a** and **2b**, respectively. The difference in the Φ_{fl} values between **2** and **3** originates from the difference in their ring systems. The imidazopyrazine rings of **3** have the aromatic character stronger than that of the imidazopyrazinone rings of **2**. Because the imidazopyrazinone ring of $M^{n+}\cdot$**2** partially has the aromatic character of the resonance structure **II**, an increase in the **II** character in $M^{n+}\cdot$**2** leads to an increased Φ_{fl} value.

2.2. X-ray crystallographic analysis of a Li^+ complex of 1b

To better understand the structural characteristics of a metal-ion complex, we examined the crystal structure of a complex of **1b** with $LiClO_4$. The crystals, $[Li(\mathbf{1b})_2(H_2O)(ROH)](ClO_4)\cdot H_2O$, obtained by recrystallization from a solution of **1b** and $LiClO_4$ containing aqueous methanol, have a tetra-coordinated tetrahedral Li^+ complex structure (Fig. 6). ROH is either methanol or H_2O with an occupancy ratio of 0.60:0.40, respectively. In the Li^+ complex, two molecules of **1b** [**1b**(A) and **1b**(B)] coordinate to Li^+ with their O10 atoms, and the remaining two sites are occupied by H_2O and ROH. Molecules **1b**(A) and **1b**(B) differ slightly in their structural character, although their bond distances and bond angles agree with each other within the 3σ level. Although the molar ratio of Li^+/**1b** (1:2) in the crystals of the $[Li(\mathbf{1b})_2(H_2O)(ROH)]$ complex differs from the 1:1 ratio for the Li^+ complexes of **2** observed in acetonitrile, formation of the O10(imidazopyrazinone)–Li^+ bond is common to the Li^+ complexes in the crystals and the solutions. The crystals also contain one molecule of water per Li^+ complex as a crystal solvent, which forms a hydrogen bond with the O10 atom of **1b**(A). The bond distances are 2.762(6) and 1.81(7) Å for O10···O(H_2O) and O10···H(H_2O), respectively, and the angle of O10···H–O(H_2O) is 155(5)°.

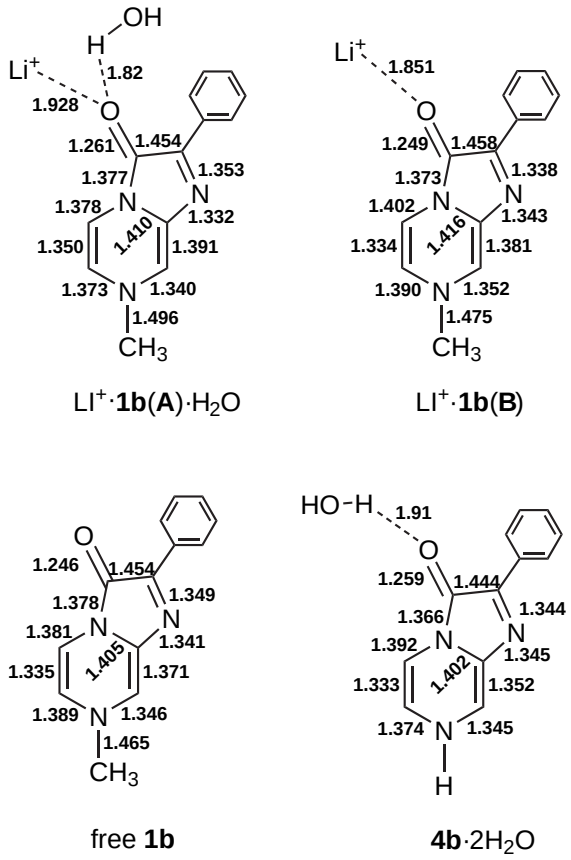

Figure 7. Selected bond distances (Å) of the imidazopyrazinone moieties in the crystals of $[Li(\mathbf{1b})_2(H_2O)(ROH)](ClO_4)\cdot H_2O$, free **1b**, and **4b**·$2H_2O$.

system, especially the C=O bond distance. The C=O bond of **1b**(A) [1.260(6) Å] is longer than that of **1b**(B) [1.249(6) Å] and is slightly longer than that of **4b**·$2H_2O$ (1.259 Å). The C=O bond of **1b**(B) is

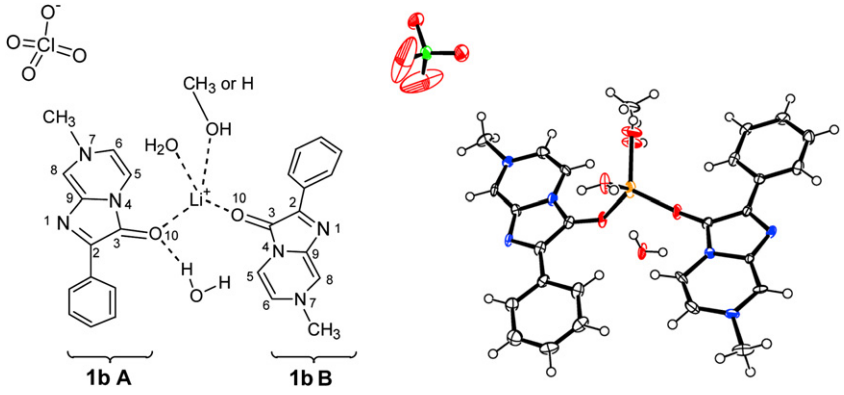

Figure 6. ORTEP drawing of $[Li(\mathbf{1b})_2(H_2O)(ROH)](ClO_4)\cdot H_2O$. Ellipsoids are drawn at the 50% probability level.

Figure 7 shows selected bond lengths of the $Li^+\cdot$**1b**(A)·H_2O and $Li^+\cdot$**1b**(B) parts of the Li^+ complex of **1b** and those of the imidazopyrazinone moieties in the crystals of free **1b** and **4b**·$2H_2O$ as reference structures.[3a,8,9] The imidazopyrazinone moiety **1b**(A) contains both the O10–Li and O10···H(H_2O) bonds, whereas **1b**(B) has only the O10–Li bond. The imidazopyrazinone moiety in the crystals of **4b**·$2H_2O$ contains the O10···H(H_2O) hydrogen bond, whereas that in the crystals of free **1b** has no bonding interaction at the O10 atom. A bonding interaction at the O10 atom of the imidazopyrazinone moiety affects the structural character of the ring slightly longer than that of free **1b** (1.246 Å). These results indicate that hydrogen bond formation at the O10 atom induces an elongation of the C=O bond in the imidazopyrazinone moiety that is greater than the elongation induced by coordinate bond formation with Li^+. The finding that the O10–Li bond of $Li^+\cdot$**1b**(A)·H_2O [1.927(10) Å] is longer than that of $Li^+\cdot$**1b**(B) [1.851(9) Å] indicates that an additional hydrogen bond with H_2O at the common O10 atom induces an elongation of the O10–Li bond. These O10–Li distances are within the range of the O–Li bond distances (1.8–2.1 Å) reported for some Li^+ complexes.[10]

2.3. Quantum chemical evaluation of the π electronic character of the metal-ion complexes of 1

To examine the structural and π electronic character of the metal-ion complexes of **2**, we performed density functional theory (DFT) calculations[11,12] on Li^+ complexes of imidazopyrazinones at the B3LYP/6-31G(d) level. We used *N*-methyl derivatives **1** for calculations instead of *N*-benzyl derivatives **2** because the former are structurally simple compounds. We optimized the geometries of free molecules of **1**, the tetra-coordinated tetrahedral Li^+ complexes {$[Li\cdot\mathbf{1}(CH_3CN)_3]^+$}, protonated species $\mathbf{1}H^+$, and 3-methoxyimidazopyrazines **3′** (Chart 2). Table 2 summarizes the calculation data: heats of formation (ΔH_f), HOMO–LUMO energy gaps (ΔE_{H-L}), summations of the Mulliken charge densities (Σq_A) of the imidazopyrazine part A, and C3–O10 and O10–Li bond distances.

3. Conclusions

In conclusion, formation of complexes of benzylimidazopyrazinones **2** with metal ions (Li^+, Mg^{2+}, Ca^{2+}, Ba^{2+}, Sc^{3+}, and La^{3+}) produced successive modulations of the spectroscopic properties in acetonitrile. The metal-ion complexes of **2** exhibited a blue shift of the absorption and fluorescence emission maxima and an increase of the fluorescence intensity compared with free molecules of **2**. Energies of the maxima of the UV/vis absorption and fluorescence emissions for the metal-ion complexes of **2** varied depending on the Lewis acidity of the metal ion. This finding indicates that an imidazopyrazinone can be used as a colorimetric and fluorometric indicator to sense the Lewis acidity of a metal ion in aprotic solutions. The fluorescence intensity change induced by the metal-ion complexation of **2** is also useful for fluorometric sensing. A strong Lewis acid–base bond also causes an increase in the formation constant (K) of a metal-ion complex. The crystal structure of a Li^+ complex of **1b** {$[Li(\mathbf{1b})_2(H_2O)(ROH)](ClO_4)\cdot H_2O$} supports the premise that the coordinate bond is formed at the O10 atom of an imidazopyrazinone in the metal-ion complex. The observed electronic and structural properties of the imidazopyrazinone moieties in the metal-ion complexes are consistent with the results of DFT calculations of the metal-ion complexes and their structurally related compounds. On the other hand, **2** did not show any spectral change caused by metal-ion complex formation in aqueous solutions, although it is necessary to have sensor characteristics in water for biological applications. To overcome the problem, we need to construct a sensor supramolecule having an imidazopyrazinone moiety included in an aprotic interior of a host structure such as a cyclodextrin and a dendrimer. Further study based on this idea is now in progress.

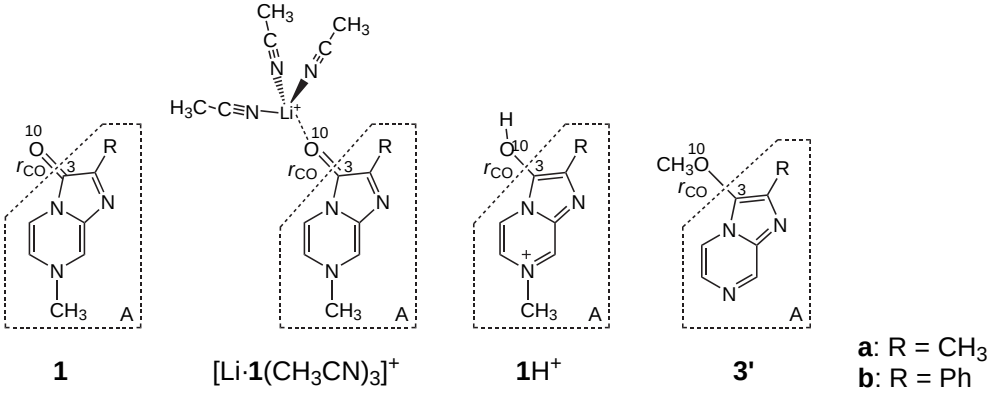

Chart 2.

Table 2
Heats of formation (ΔH_f), HOMO–LUMO energy gaps (ΔE_{H-L}), summations of the Mulliken charge densities of the imidazopyrazine part A (Σq_A), and C3–O10 and O–Li bond distances for **1**, $[Li\cdot\mathbf{1}(CH_3CN)_3]^+$, $\mathbf{1}H^+$, and **3′** in the gas phase, obtained using DFT at the B3LYP/6-31G(d) level

Compounds	ΔH_f/hartree	ΔE_{H-L}/eV	Σq_A[a]	C3–O10[b]/Å	O10–Li[c]/Å
1a	−549.7	3.20	+0.489	1.230	—
$[Li\cdot\mathbf{1a}(CH_3CN)_3]^+$	−955.5	3.41	+0.781	1.256	1.845
$\mathbf{1a}H^+$	−550.1	3.90	+1.123	1.333	—
3a′	−549.7	4.68	+0.227	1.355	—
1b	−741.5	2.85	+0.498	1.232	—
$[Li\cdot\mathbf{1b}(CH_3CN)_3]^+$	−1147.2	3.10	+0.781	1.256	1.855
$\mathbf{1b}H^+$	−741.8	3.35	+1.136	1.332	—
3b′	−741.4	4.38	+0.223	1.355	—

[a] Mulliken charge densities of the imidazopyrazine part A in Chart 2.
[b] Bond distances of C3–O10.
[c] Bond distances of O10–Li.

The O10–Li bond distance (1.855 Å) of $[Li\cdot\mathbf{1b}(CH_3CN)_3]^+$ is similar to that (1.851 Å) of the $Li^+\cdot\mathbf{1b}$(B) part in the crystal of $[Li(\mathbf{1b})_2(H_2O)(ROH)](ClO_4)\cdot H_2O$. The order of the ΔE_{H-L} values is $\mathbf{1}<[Li\cdot\mathbf{1}(CH_3CN)_3]^+<\mathbf{1}H^+<\mathbf{3}'$, which reproduces the order of the energies (E_{ab}) estimated from λ_{ab} for the lowest energy absorption bands of **2**, $Li^+\cdot\mathbf{2}$, $\mathbf{2}H^+$, and **3**. The ΔE_{H-L} values, the Σq_A values, and the C3–O10 bond distances also show the order $\mathbf{1}<[Li\cdot\mathbf{1}(CH_3CN)_3]^+<\mathbf{1}H^+$. An increase in the Σq_A value and an elongation of the C3–O10 bond correspond to an increase in the contribution of the character of the resonance structure **II** in Scheme 1 more than that of **I**, because **II** contains the positive imidazopyrazinium moiety with the C3–O10 single bond. Therefore, these DFT calculations support the π electronic characteristics of the imidazopyrazinone ring of $M^{n+}\cdot\mathbf{2}$ explained using the resonance structures **I** and **II**.

4. Experimental section

4.1. General

Melting points were measured using a Yamato MP-21 apparatus. IR spectra were measured with a Horiba FT-720 spectrometer. Electron impact (EI) and fast atom bombardment (FAB) mass spectrometry (MS) were performed using JEOL JMS-600 and Thermo Fisher Scientific TSQ 700 mass spectrometers, respectively. High-resolution (HR) EIMS data were recorded using a Bruker-Daltonics APEX III mass spectrometer. Elemental analysis was performed at the Research Centre for Giant Molecules, Graduate School of Science, Tohoku University. ^{1}H NMR spectra were recorded on a JEOL GX-270 instrument (270 MHz). UV/vis absorption spectra were measured with a Varian Cary 50 spectrophotometer.

Fluorescence spectra were recorded on a JASCO FP-6500 fluorescence spectrophotometer (excitation and emission band passes, 3 nm; scan speed, 500 nm/min). Fluorescence quantum yields were determined by comparing the corrected fluorescence spectra with that of quinine sulfate in 0.10 M H_2SO_4 (Φ_{fl}=0.55, λ_{ex} 355 nm) as the standard.[13] Spectroscopic measurements were made in a quartz cuvette (1 cm path length) at 25±1 °C. Spectral-grade acetonitrile was used for measurements of UV/vis absorption and fluorescence. Quantum chemical calculations were performed using the Gaussian 03 program[11] on the computer system of the Information Technology Center of UEC. We used DFT with Beck's three-parameter functional combined with Lee, Yang, and Parr's correlation functional (B3LYP) along with a 6-31G(d) basis set.[12]

4.2. Preparation of imidazopyrazinone derivatives

*4.2.1. 7-Benzyl-2-methylimidazo[1,2-a]pyrazin-3(7H)-one (**2a**) and 3-benzyloxy-2-methylimidazo[1,2-a]pyrazine (**3a**).* K_2CO_3 (822 mg, 6.12 mmol) and benzyl chloride (0.35 mL, 3.1 mmol) were added to a solution of 2-methylimidazo[1,2-*a*]pyrazin-3(7*H*)-one hydrochloride (306 mg, 1.65 mmol) in DMF (2 mL) at room temperature under Ar. After stirring overnight, water was added to the reaction mixture, and the products were extracted with ethyl acetate. The organic layer was dried over anhydrous Na_2SO_4 and concentrated in vacuo. The yellow residue was purified by silica-gel column chromato graphy (chloroform/methanol=20:1), yielding **2a** (106 mg, 27%) as a yellow powder and **3a** (51 mg, 13%) as colorless cubes. Compound **2a**: mp 198 °C (dec); ^{1}H NMR (270 MHz, CD_3OD) δ 7.99 (s, 1H), 7.3–7.5 (m, 6H), 6.98 (dd, *J*=1.3, 5.9 Hz, 1H), 5.11 (s, 2H), 2.42 (s, 3H); IR (KBr) 3093, 3076, 2925, 2360, 1684, 1599, 1558, 1498 cm^{-1}; MS (EI) *m*/*z* 239 (M^+, 78), 120 (26), 91 (100); HRMS (EI) calcd for $C_{14}H_{13}N_3O$: 239.1059, found: 239.1053. Anal. Calcd for $C_{14}H_{13}N_3O\cdot 1/5H_2O$: C, 69.23; H, 5.56; N, 17.30. Found: C, 69.49; H, 5.65; N, 16.99. Compound **3a**: mp 76–77 °C; ^{1}H NMR (270 MHz, $CDCl_3$) δ 8.82 (d, *J*=1.6 Hz, 1H), 7.68 (d, *J*=4.3 Hz, 1H), 7.56 (dd, *J*=1.3, 4.6 Hz, 1H), 7.3–7.4 (m, 5H), 5.13 (s, 2H), 2.38 (s, 3H); IR (KBr) 3035, 2941, 2360, 1616, 1552, 1496 cm^{-1}; MS (EI) *m*/*z* 239 (M^+, 70), 120 (40), 91 (100); HRMS (EI) calcd for $C_{14}H_{13}N_3O$: 239.1059, found: 239.1052.

*4.2.2. 7-Benzyl-2-phenylimidazo[1,2-a]pyrazin-3(7H)-one (**2b**) and 3-benzyloxy-2-phenylimidazo[1,2-a]pyrazine (**3b**).* Compounds **2b** and **3b** were prepared from 2-phenylimidazo[1,2-*a*]pyrazin-3(7*H*)-one by a procedure analogous to that used for **2a** and **3a**. Compound **2b** (yield 31%): red powder, mp 192 °C (dec); ^{1}H NMR (270 MHz, CD_3OD) δ 8.44 (m, 2H), 8.12 (d, *J*=1.3 Hz, 1H), 7.58 (d, *J*=5.9 Hz, 1H), 7.3–7.5 (m, 8H), 7.01 (dd, *J*=1.6, 5.9 Hz, 1H), 5.17 (s, 2H); IR (KBr) 3093, 3060, 2920, 1668, 1591, 1496 cm^{-1}; MS (EI) *m*/*z* 301 (M^+, 100), 182 (87), 91 (92); HRMS (EI) calcd for $C_{19}H_{15}N_3O$: 301.1215, found: 301.1209. Anal. Calcd for $C_{19}H_{15}N_3O\cdot 1/3H_2O$: C, 74.25; H, 5.14; N, 13.67. Found: C, 74.45; H, 5.11; N, 13.46. Compound **3b** (yield 19%): colorless powder, mp 105–106 °C; ^{1}H NMR (270 MHz, $CDCl_3$) δ 8.94 (d, *J*=1.6 Hz, 1H), 8.15 (m, 2H), 7.67 (d, *J*=4.6 Hz, 1H), 7.2–7.5 (m, 9H), 5.11 (s, 2H); IR (KBr) 3030, 2360, 1549, 1489 cm^{-1}; MS (EI) *m*/*z* 301 (M^+, 70), 210 (25), 182 (100), 91 (39); HRMS (EI) calcd for $C_{19}H_{15}N_3O$: 301.1215, found: 301.1211.

4.3. Formation constants *K* for the 1:1 metal–ion complexes of 2

Formation constants [*K* in Eq. 1] for the 1:1 complexation of **2** with Li^+, Mg^{2+}, Ca^{2+}, and Ba^{2+} were estimated by analyses of UV/vis absorption spectra of **2** in acetonitrile in the absence and the presence of these metal ions at various concentrations at 25 °C (Fig. 4). The observed spectral changes were analyzed by Eq. 2.[7] The value A_0 is the absorbance of **2** at a chosen wavelength in the absence of a metal ion (M^{n+}). A_{obs} is the absorbance at the chosen wavelength after addition of M^{n+}. The difference between A_{obs} and A_0 is given by:

$$A_{obs}-A_0 = 0.5\Delta\varepsilon\left([\mathbf{2}]+\left[M^{n+}\right]+1/K-\left\{\left([\mathbf{2}]+\left[M^{n+}\right]+1/K\right)^2-4[\mathbf{2}]\left[M^{n+}\right]\right\}^{1/2}\right), \quad (2)$$

where [**2**] and [M^{n+}] are the initial concentrations of **2** and M^{n+}, respectively, and $\Delta\varepsilon$ is the difference in the molar absorptivity between **2** and the complex ($M^{n+}\cdot$**2**) at the chosen wavelength. The (A_{obs}–A_0) values were plotted against [M^{n+}], as shown in Figure 4C and D. The data were analyzed using a nonlinear least squares curve fitting Eq. 2, which provided the *K* values summarized in Table 1.

4.4. X-ray crystallographic analysis of a Li^+ complex of 1b

Single crystals of [Li(**1b**)$_2$(H_2O)(ROH)](ClO_4)·H_2O (R=H and CH_3) were obtained as red cubes by slow evaporation from a solution of **1b** and $LiClO_4$ in a mixture of aqueous methanol, diethyleneglycol dimethyl ether, and chloroform. Diffraction data were collected with a Rigaku RAXIS-CS Imaging Plate diffractometer using graphite monochromated Mo Kα radiation (λ=0.71073 Å) at 100 K. The structure was solved by direct methods using the program SIR-97.[14] Refinements were performed by a least squares method on F^2 using the program SHELXL-97.[15]

Crystal data are as follows: $C_{13.3}H_{14.6}Cl_{0.5}Li_{0.5}N_3O_{4.5}$, *M*=309.71, triclinic, space group *P*-1, *a*=7.5848(4), *b*=11.9476(6), *c*=16.2294(9) Å, α=87.698(2)°, β=80.491(2)°, γ=84.428(1)°, *V*=1443.2(1) Å^3, *Z*=4, D_x=1.425 Mg m^{-3}, μ=0.196 mm^{-1}, 6545 unique data, final $R(F)$=0.1068, $wR(F^2)$=0.2204 for 432 observed data [$I>2\sigma(I)$]. The crystallographic data have been deposited at the CCDC, 12 Union Road, Cambridge CB2 1EZ, UK (CCDC 761060).

Acknowledgements

We gratefully acknowledge financial supports in the form of Grants-in-Aid [Nos. 20044027 and 21021025 (Priority Area 'New Frontiers in Photochromism' No. 471), 21108520 (Innovative Area 'pi-Space' No. 2007), 20044027 (Scientific Research B), and 21655016 (Challenging Exploratory Research) for H.I.] and in the form of the Cooperation for Innovative Technology and Advanced Research in Evolutional Area (CITY AREA) program from the Ministry of Education, Culture, Sports, Science and Technology of Japan. H.I. also thanks financial supports from the Shorai Foundation, the Iketani Foundation, and the Mazda Foundation for Science and Technology. We acknowledge technical assistance in computing the quantum chemical calculations from the Information Technology Center of UEC. We also thank Professor K. Mizuno (Osaka Prefecture University) for his generous considerations.

References and notes

1. (a) Bamfield, P. *Chromic Phenomena—Technological Applications of Colour Chemistry*; RSC: Cambridge, 2001; (b) Zollinger, H. *Color Chemistry: Syntheses, Properties, and Applications of Organic Dyes and Pigments*, 3rd ed.; Wiley-VCH: Weinheim, 2003.
2. Reviews: (a) Goto, T. *Pure Appl. Chem.* **1968**, *17*, 421–441; (b) Goto, T.; Kishi, Y. *Angew. Chem., Int. Ed. Engl.* **1968**, *7*, 407–488; (c) Johnson, F. H.; Shimomura, O. *Methods Enzymol.* **1978**, *57*, 271–291; (d) Ohmiya, Y.; Hirano, T. *Chem. Biol.* **1996**, *3*, 337–347; (e) Shimomura, O. *Bioluminescence: Chemical Principles and Methods*; World Scientific: Singapore, 2006.
3. (a) Nakai, S.; Yasui, M.; Nakazato, M.; Iwasaki, F.; Maki, S.; Niwa, H.; Ohashi, M.; Hirano, T. *Bull. Chem. Soc. Jpn.* **2003**, *76*, 2361–2387; (b) Fujio, S.; Hashizume, D.; Takamuki, Y.; Yasui, M.; Iwasaki, F.; Maki, S.; Niwa, H.; Ikeda, H.; Hirano, T. *Tetrahedron Lett.* **2004**, *45*, 8531–8534; (c) Takamuki, Y.; Maki, S.; Niwa, H.; Ikeda, H.; Hirano, T. *Chem. Lett.* **2004**, *33*, 1484–1485; (d) Takamuki, Y.; Maki, S.; Niwa, H.; Ikeda, H.; Hirano, T. *Tetrahedron* **2005**, *61*, 10073–10080.

4. A preliminary report on this work: Sekiguchi, T.; Maki, S.; Niwa, H.; Ikeda, H.; Hirano, T. *Tetrahedron Lett.* **2004**, *45*, 1065–1069.
5. 7-Benzyl structure of **2** is useful for designing an analogous molecular structure having plural imidazopyrazinone moieties, such as 1,2- and 1,3-bis(imidazopyrazinonylmethyl)benzenes.[4]
6. (a) Fukuzumi, S.; Ohkubo, K. *Chem.—Eur. J.* **2000**, *6*, 4532–4535; (b) Fukuzumi, S.; Ohkubo, K. *J. Am. Chem. Soc.* **2002**, *124*, 10270–10271; (c) Ohkubo, K.; Menon, S. C.; Orita, A.; Otera, J.; Fukuzumi, S. *J. Org. Chem.* **2003**, *68*, 4720–4726.
7. Schneider, H. J.; Yatsimirsky, A. *Principles and Methods in Supramolecular Chemistry*; John Wiley: Chichester, UK, 2000.
8. The crystals of free **1b** contain two crystallographically independent molecules with the 1:1 ratio in the asymmetric unit.[3a] The two crystallographically independent molecules of **1b** show the same C=O distance (1.246 Å).
9. Devillers, I.; de Wergifosse, B.; Bruneau, M.-P.; Tinant, B.; Declercq, J.-P.; Touillaux, R.; Ress, J.-F.; Marchand-Brynaert, J. *J. Chem. Soc., Perkin Trans. 2* **1999**, 1481–1487.
10. (a) Olsher, U.; Izatt, R. M.; Bradshaw, J. S.; Dalley, N. K. *Chem. Rev.* **1991**, *91*, 137–164; (b) Setzer, W. N.; Schleyer, P. v. R. In *Advances in Organometallic Chemistry*; Stone, F. G. A., West, R., Eds.; Academic: Orlando, FL, 1985; Vol. 24, pp 353–451.
11. Frisch, M. J.; Trucks, G. W.; Schlegel, H. B.; Scuseria, G. E.; Robb, M. A.; Cheeseman, J. R.; Montgomery, J. A., Jr.; Vreven, T.; Kudin, K. N.; Burant, J. C.; Millam, J. M.; Iyengar, S. S.; Tomasi, J.; Barone, V.; Mennucci, B.; Cossi, M.; Scalmani, G.; Rega, N.; Petersson, G. A.; Nakatsuji, H.; Hada, M.; Ehara, M.; Toyota, K.; Fukuda, R.; Hasegawa, J.; Ishida, M.; Nakajima, T.; Honda, Y.; Kitao, O.; Nakai, H.; Klene, M.; Li, X.; Knox, J. E.; Hratchian, H. P.; Cross, J. B.; Bakken, V.; Adamo, C.; Jaramillo, J.; Gomperts, R.; Stratmann, R. E.; Yazyev, O.; Austin, A. J.; Cammi, R.; Pomelli, C.; Ochterski, J. W.; Ayala, P. Y.; Morokuma, K.; Voth, G. A.; Salvador, P.; Dannenberg, J. J.; Zakrzewski, V. G.; Dapprich, S.; Daniels, A. D.; Strain, M. C.; Farkas, O.; Malick, D. K.; Rabuck, A. D.; Raghavachari, K.; Foresman, J. B.; Ortiz, J. V.; Cui, Q.; Baboul, A. G.; Clifford, S.; Cioslowski, J.; Stefanov, B. B.; Liu, G.; Liashenko, A.; Piskorz, P.; Komaromi, I.; Martin, R. L.; Fox, D. J.; Keith, T.; Al-Laham, M. A.; Peng, C. Y.; Nanayakkara, A.; Challacombe, M.; Gill, P. M. W.; Johnson, B.; Chen, W.; Wong, M. W.; Gonzalez, C.; Pople, J. A. *Gaussian 03, Revision C.02*; Gaussian: Wallingford, CT, 2004.
12. (a) Becke, A. D. *J. Chem. Phys.* **1993**, *98*, 5648–5652; (b) Lee, C.; Yang, W.; Parr, R. G. *Phys. Rev. B* **1988**, *37*, 785–789; (c) Stephens, P. J.; Devlin, F. J.; Chabalowski, C. F.; Frisch, M. J. *J. Phys. Chem.* **1994**, *98*, 11623–11627.
13. Eaton, D. F. *Pure Appl. Chem.* **1988**, *60*, 1107–1114.
14. Altomare, A.; Burla, M. C.; Camalli, M.; Cascarano, G. L.; Giacovazzo, C.; Guagliardi, A.; Moliterni, A. G.; Polidori, G.; Spagna, R. *J. Appl. Crystallogr.* **1999**, *32*, 115–119.
15. Sheldrick, G. M. *Acta Crystallogr., Sect. A* **2008**, *64*, 112–122.